ORIGINALS ORIGINALARBEITEN

Softwood heating in radio frequency fields

**Ken Watanabe · Alhassan Abubakari ·
Ciprian Lazarescu · Stavros Avramidis**

Abstract The aim of this study was to investigate the heating rate of lodgepole pine (*Pinus contorta*) and western red cedar (*Thuja plicata*) during radio frequency (RF) heating. Wood specimens ($40 \times 150 \times 1000$ mm^3) with various moisture content and power density were heated using a laboratory size RF dryer at a frequency of 40.7 MHz, until shell temperature reached 56 °C that is approved as a lethal temperature for phytosanitation. Heating rate was positively correlated with power density and negatively correlated with moisture content. The ratio of heating rate to power density had a negative correlation with moisture content and density in both pine and cedar. The regression lines for moisture content had good coefficient of determination (R^2) values of 0.63 and 0.61 °C m^3/min kW (pine), 0.50 and 0.55 °C m^3/min kW (red cedar) in both shell and core, respectively. The results demonstrate that the ratio of heating rate to power density is a useful parameter to estimate heating rate. The derived empirical equations made possible the calculation of the heating rate within test conditions applied to this study. The initial temperature rise in shell and core allowed a rather accurate determination of local power density. One dimensional mathematical model to describe the heating rate of wood during RF heating that was derived from the governing heat transfer equation combined with internal heat generation was developed and verified. The model using local power density had high R^2 of 0.71 and 0.93 in both shell and core, respectively, indicating that the model was able to predict heating rate of wood with various moisture content under the known power density distribution.

K. Watanabe · A. Abubakari · C. Lazarescu · S. Avramidis (✉)
Department of Wood Science, University of British Columbia,
2424 Main Mall, Vancouver, BC, V6T 1Z4, Canada
e-mail: stavros.avramidis@ubc.ca

Erhitzung von Nadelholz in Hochfrequenzfeldern

Zusammenfassung Ziel dieser Studie war es, die Aufheizrate von Lodgepole Kiefer (*Pinus contorta*) und Western Red Cedar (*Thuja plicata*) bei Hochfrequenzerwärmung (RF) zu untersuchen. Holzprüfkörper ($40 \times 150 \times 1000$ mm^3) mit unterschiedlicher Holzfeuchte und Leistungsdichte wurden mit einem Labor-Hochfrequenztrockner bei einer Frequenz von 40,7 MHz erwärmt, bis die Oberflächentemperatur 56 °C erreicht hatte. Diese gilt im phytosanitären Bereich als letale Temperatur. Die Aufheizrate korrelierte positiv mit der Leistungsdichte und negativ mit der Holzfeuchte. Das Verhältnis von Aufheizrate zu Leistungsdichte korrelierte sowohl bei Kiefer als auch bei Western Red Cedar negativ mit der Holzfeuchte und der Dichte. Die Regressionsgeraden mit der Holzfeuchte wiesen gute Bestimmtheitsmaße (R^2) von 0,63 und 0,61 °C m^3/min kW für Kiefer und 0,50 und 0,55 °C m^3/min kW für Red Cedar an der Oberfläche bzw. im inneren Querschnittsbereich auf. Die Ergebnisse zeigen, dass das Verhältnis von Aufheizrate zu Leistungsdichte ein nützlicher Parameter zur Schätzung der Aufheizrate ist. Die hergeleiteten empirischen Gleichungen ermöglichten die Berechnung der Aufheizrate unter den in dieser Studie gewählten Versuchsbedingungen. Der anfängliche Temperaturanstieg im äußeren und inneren Querschnittsbereich erlaubte eine ziemlich genaue Bestimmung der örtlichen Leistungsdichte. Ein eindimensionales mathematisches Modell zur Beschreibung der Aufheizrate von Holz während der Hochfrequenzerwärmung, hergeleitet auf Basis der geltenden Wärmeübergangsgleichung in Verbindung mit der internen Wärmeentwicklung, wurde entwickelt und verifiziert. Das Modell, das die lokale Leistungsdichte verwendet, ergab hohe R^2-Werte von 0,71 und 0,93 im äußeren bzw. inneren Querschnittsbereich. Dies weist darauf hin, dass das Model in der Lage ist, die Aufheizrate von Holz bei

unterschiedlicher Holzfeuchte und bei bekannter Leistungs-dichteverteilung vorherzusagen.

1 Introduction

The introduction and spread of invasive non-native species of pests (beetles/fungi and nematodes) is a major threat to the health and biological diversity of rural and urban areas (Perrings et al. 2005; Work et al. 2005; Tkacz 2002) thus, treatment of all wood used in packaging for global trade is required (FAO 2002). Although phytosanitary certification is required for many products, logs, lumber and other wood commodities are still not strictly regulated however, this will likely change in the near future. Currently, only two treatments are approved: (a) fumigation with methyl bromide that has a detrimental effect on the ozone layer and therefore its use has been phased out (UNEP 2000) and (b) heat treatment (HT) that consists of achieving a wood inside temperature of 56 °C for at least 30 minutes. Conventional heating has mainly been used to meet the HT specification that is not always economically feasible, especially for large size timbers or logs. Alternative methods that can heat the wood fast and efficiently with no degrade are much more desirable.

Microwave heating is considered to be effective for the dis-infestation of green lumber (Henin et al. 2008; Nzokou et al. 2008; Fleming et al. 2002, 2004). However, absorption depth is inversely proportional to frequency so the depth of penetration is low and microwave treatment is not applicable for large size materials, such as logs, timber and other wood commodities. On the other hand radio frequency (RF) heating may be an alternative treatment for large size timbers and logs especially in a batch process. Dielectric materials such as wood can be selectively heated in an RF electromagnetic field mostly because of the ionic conduction in the cell walls and lumens. This situation will result in rapid heat generation within the body of a piece of lumber and will considerably increase its internal temperature (Avramidis et al. 1994). Specific studies, aiming to eradicate either nematodes or wood decay fungi using an RF treatment, have been recently conducted (Tubajika et al. 2007; Fang et al. 2001; Dwinell et al. 1994; Lazarescu et al. 2009).

The knowledge of wood heating rate in an RF field is essential for engineering and process design and optimization reasons. Knowledge of the heating rate affects the level of the power input and the quality of the product upon reaching the desired temperature level. Too fast heating may result in internal defects and too low may result in excessive heating times both making the process non-economical. Nonetheless, little has been reported on the heating rate within RF fields because RF technology has not been used much for solely heating wood, but it has been used for drying wood in combination with vacuum (Koumoutsakos et al. 2001a;

Perré and Turner 1997, 1999). The purpose of this study was to investigate the RF heating rate of wood as a function of moisture content and power density. Furthermore, numerical modeling of heating rate was developed and validated with experimental results.

2 Materials and methods

Sixty-six lodgepole pine (*Pinus contorta*) and seventy-four western red cedar (*Thuja plicata*) lumbers, 40×150 mm^2 in cross section and 1500 mm long, were prepared from healthy green boards obtained from an interior BC sawmill. Two 20 mm thick sections were cut at a distance of more than 200 mm from each end, thus resulting in a specimen 1 meter long. The two sections were immediately weighed with a digital balance to 0.01 g and dried in an oven at 103 ± 2 °C for one day. The oven-dry weight was measured, and moisture content was calculated. The mean moisture content value of the two sections was used to calculate the mean moisture content of each specimen based on weight. Every specimen was weighed prior to each RF heating run so that its average moisture content and density could be obtained.

A laboratory size RF dryer with horizontal electrode plates was used in this study. An RF oscillator generated the electromagnetic field that operated at a stabilized frequency of 40.7 MHz and had a maximum output of 8 kW. Matching networks were used to ensure efficient transfer of energy into the wood. Transmission sections with forward and reverse reflectometers were used to monitor the energy transferred to the specimen so that the desired RF power was able to be maintained during heating.

Two small holes were drilled in a specimen, one from the middle of the side face to the geometric center (called "core") and the other 50 mm from the end of the side face to 3.5 mm deep from surface (called "shell"), respectively. Fiber-optic electrode probes (FISO Technologies Inc., Quebec, Canada) were inserted tightly into the holes in order to measure their end-point temperature. One or two specimens were put in the dryer at a time. When two specimens were heated, the pair was carefully selected to keep their average moisture content close so that RF field variation between two specimens could be reduced. Various power densities that ranged between 30 and 200 kW/m^3 were applied to specimens at numerous moisture content levels and kept constant during RF heating. Specimens were heated until both shell and core temperature reached the target temperature of 56 °C that is approved as a lethal temperature for phytosanitation (FAO 2002).The specimens were weighed after RF heating to calculate moisture loss. Then internal checking inside cross section adjacent to core was observed by cutting specimen in half perpendicular to grain.

Dielectric materials including wood store a part of the electric energy and convert the energy into heat. The heat generated per unit volume is known as power density and can be calculated as (Torgovnikov 1993):

$$\Phi = 2\pi f \varepsilon_0 E^2 \varepsilon'' \qquad (1)$$

where Φ is the power density (W/m^3), f is the frequency (Hz), ε_0 is the dielectric constant of free space (8.854 farad/m), E is the electric field intensity (V/m), and ε'' is the dielectric loss factor. In the case of an amplifier, power density is an externally controllable variable through a matching network, and power density was able to be maintained constant in this study.

If heat transfer and heat loss due to moisture evaporation are not taken into account, the equation to calculate the heating rate inside wood, resulting from the conversion of high frequency energy from the electric field to heat, can be expressed as (Nelson and Kraszewski 1990):

$$\frac{\partial T}{\partial t} = \frac{\Phi}{\rho C_p} \qquad (2)$$

where T is the temperature (°C), t is the time (s), ρ is the density (kg/m^3), C_p is the specific heat (J/kg °C).

The specific heat of wood depends on the temperature and moisture content, and should be distinguished between below and above fiber saturation point. The specific heat of dry wood C_{p0} and the specific heat of wood below fiber saturation C_p' are approximately related to temperature (Simpson and TenWolde 1999):

$$C_{p0} = 0.1031 + 0.003867(T + 273) \qquad (3)$$

$$C_p' = \frac{(C_{p0} + 0.01 M C_{pw})}{1 + 0.01M} + A_c \qquad (4)$$

where M is moisture content (%), C_{pw} is the specific heat of water, A_c is the adjustment factor derived from:

$$A_c = M(b_1 + b_2 T + b_3 M) \qquad (5)$$

with $b_1 = -0.06191$, $b_2 = 2.36 \times 10^{-4}$, and $b_3 = -1.33 \times 10^{-4}$. The moisture above fiber saturation contributes to specific heat according to the simple rule of mixtures, and thus the specific heat of wood above fiber saturation C_p is expressed by:

$$C_p = C_p' R_w + C_{pw}(1 - R_w) \qquad (6)$$

where R_w is the ratio of the weight of wood at fiber saturation point divided by the total weight of wood.

Once the thermal energy is generated inside wood, it moves by conduction. Assuming that moisture is constant during RF heating, wood temperature as a function of time at any locations is governed by a general energy balance equation (Koumoutsakos et al. 2001b):

$$\rho C_p \frac{\partial T}{\partial t} = K \frac{\partial^2 T}{\partial x^2} + \Phi \qquad (7)$$

where K is the thermal conductivity of wood (J/m s °C) and x is the coordinate originating from the wood center (m).

In RF heating, thermal energy is transferred from the wood surface to air by natural convection as described by the following boundary heat flux equation:

$$-K \frac{\partial T}{\partial t} = h[T_s - T_\infty] \qquad (8)$$

where h is the surface heat transfer coefficient (J/m^2 s °C), T_s is the surface temperature (°C) and T_∞ is the ambient temperature (°C). The surface heat transfer coefficient of vertical plate with natural convection of laminar flow can be simplified using the abbreviated empirical equation based on the Fishenden and Saunders equation (Itoh 2004; Khalifa 2001):

$$h = 2.51C \left(\frac{T_s - T_\infty}{L} \right)^{0.25} \qquad (9)$$

where C is the coefficient that depends on the shape of specimen and equals 0.56 for natural convection from vertical plate. L is the characteristic length (m).

When initial temperature, initial moisture content, density, transverse thermal conductivity, surface heat transfer coefficient, ambient temperature and power density that are all measured except transverse thermal conductivity is provided, (7) in combination with (6) and (8) can be solved numerically. Transverse thermal conductivity of 0.10 J/m s °C was used from literature data (Simpson and Ten-Wolde 1999). By developing the simulation model of this study, (6), (7) and (8) were replaced by one dimensional finite difference equations (Shida 1993), considering the following assumptions:

(1) Moisture content and thermal conductivity were constant during RF heating.
(2) Moisture content within specimen was uniform, and thus power density was also uniform.
(3) Heat conduction occurred along horizontal direction within cross section.
(4) Heat on surface was transferred by natural convection.
(5) Longitudinal direction of lumber was thermally semi-infinite.

Wood temperature as a function of time and depth from surface was obtained using an iterative procedure with a simulation time step of 1 second.

3 Results and discussion

A wide range of moisture content and density was achieved. The moisture content of pine and red cedar was ranging from 21 to 158% and 17 to 133%, respectively. The density of pine and red cedar was ranging from 430 to 839 kg/m^3 and 353 to 766 kg/m^3, respectively.

298

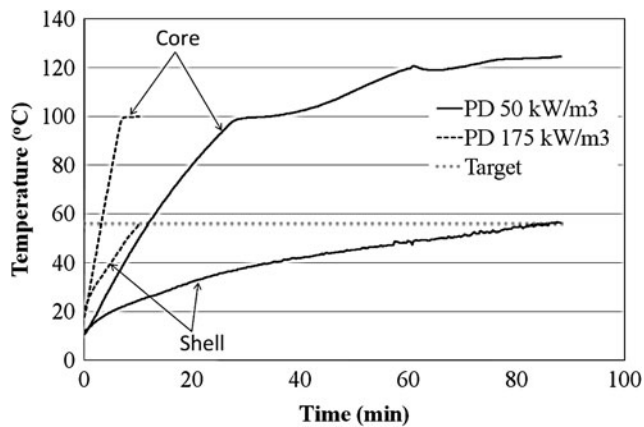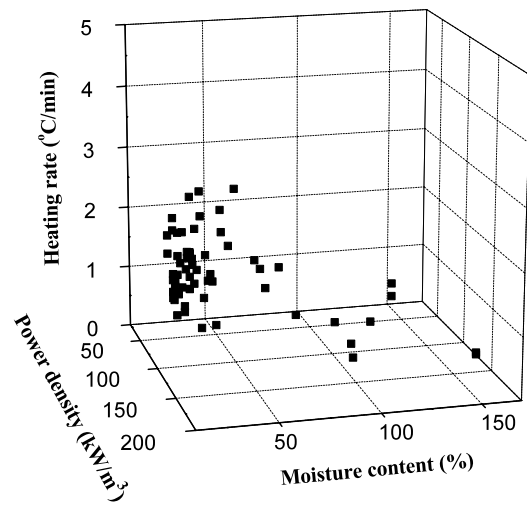Eur. J. Wood Prod. (2011) 69: 295–301

Fig. 1 Typical temperature evolution of shell and core with power densities of 50 and 175 kW/m³. The initial moisture content of the specimen was 34%
Abb. 1 Typische Temperaturentwicklung im äußeren und inneren Querschnittsbereich mit Leistungsdichten von 50 und 175 kW/m³. Die anfängliche Holzfeuchte der Prüfkörper betrug 34 %
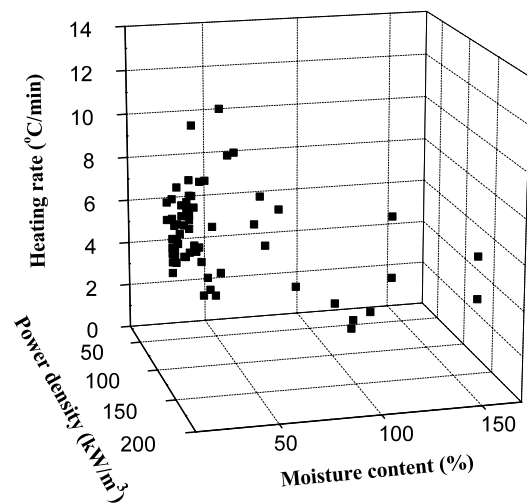
Typical shell and core temperature rise for power densities of 50 and 175 kW/m³ is depicted in Fig. 1. It is clear that there was a strong positive correlation between heating rate and power density level. In less than 15 minutes of field exposure, the wood temperature with power densities of 175 kW/m³ reached the target temperature of 56 °C in both core and shell, whereas the shell temperature with power density of 50 kW/m³ took 86 minutes to reach the target temperature. In both power densities, the shell temperature increased much slower than core temperature mainly due to heat transfer from the surface to the ambient environment. When the shell temperature with power density of 50 kW/m³ reached the target temperature the core temperature was over 120 °C. Core temperatures over 120 °C can be seen in both pine and red cedar where internal checking was often observed. In terms of industrial application of RF heating for pasteurization, a technology to prevent heat transfer on surface (e.g. thermal insulation environment or radiation heating) may be required for shell temperature to achieve the target temperature before core temperature reaches 120 °C.

RF heating caused a certain amount of moisture loss. Average moisture loss of pine and red cedar was 20.5 and 18.1%, respectively. However the core remained wetter than the shell after RF heating and drastic drying of core did not appear to happen. Therefore internal checking could result from high temperature that causes high vapor pressure and reduced cell-wall strength.

Figures 2 and 3 showed the heating rate of pine and red cedar, respectively, as a function of moisture content and power density. The heating rate varied widely, depending on moisture content and power density, and appeared to be negatively correlated with moisture content in both shell and core.

(a)

(b)

Fig. 2 Heating rate of pine in shell (**a**) and core (**b**) as a function of moisture content and power density
Abb. 2 Aufheizrate von Kiefer im (**a**) äußeren und (**b**) inneren Querschnittsbereich in Abhängigkeit der Holzfeuchte und der Leistungsdichte

As a first step of the evaluation of heating rate, out of the consideration of the heat transfer and conduction, heating rate is theoretically proportional to power density (2). The ratio of heating rate to power density was introduced as a parameter to cancel the influence of the latter, so that the effect of moisture content and density upon heating rate can be evaluated. Figure 4 shows the negative correlation between moisture content and the ratio of heating rate to power density of pine and red cedar. The regression lines had good coefficient of determination (R^2) values of 0.63 and 0.61 °C m³/min kW (pine), 0.50 and 0.55 °C m³/min kW (red cedar) in both shell and core, respectively. The results indicate that the ratio of heating rate to power density is a useful parameter and that the heating rate can be estimated
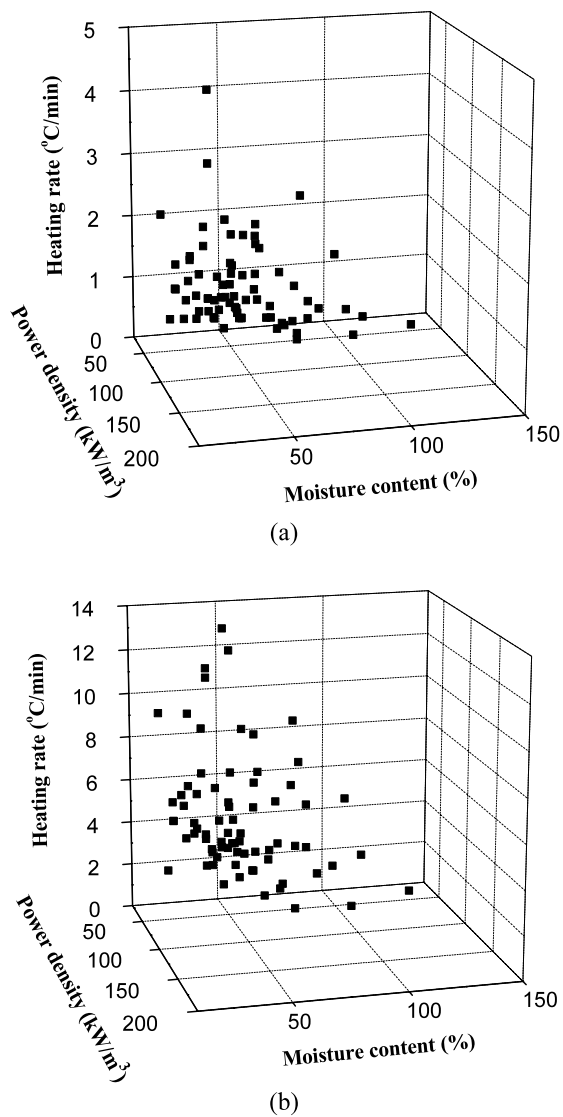
(a)

(b)

Fig. 3 Heating rate of red cedar in shell (**a**) and core (**b**) as a function of moisture content and power density
Abb. 3 Aufheizrate von Red Cedar im (**a**) äußeren und (**b**) inneren Querschnittsbereich in Abhängigkeit der Holzfeuchte und der Leistungsdichte

Fig. 4 Relationship between moisture content and the ratio of heating rate to power density of lodgepole pine (**a**) and western red cedar (**b**)
Abb. 4 Beziehung zwischen Holzfeuchte und dem Verhältnis von Aufheizrate zu Leistungsdichte bei (**a**) Lodgepole Kiefer und (**b**) Western Red Cedar

as a function of moisture content by means of the product of this parameter and power density.

Figure 5 shows the relationship between density and the ratio of heating rate to power density. The R^2 value showed a good agreement in both pine and red cedar, demonstrating that density is also a useful and practical property of wood to estimate heating rate, as well as moisture content. The derived empirical equations in Figs. 4 and 5 made possible the calculation of the heating rate within test conditions applied to this study.

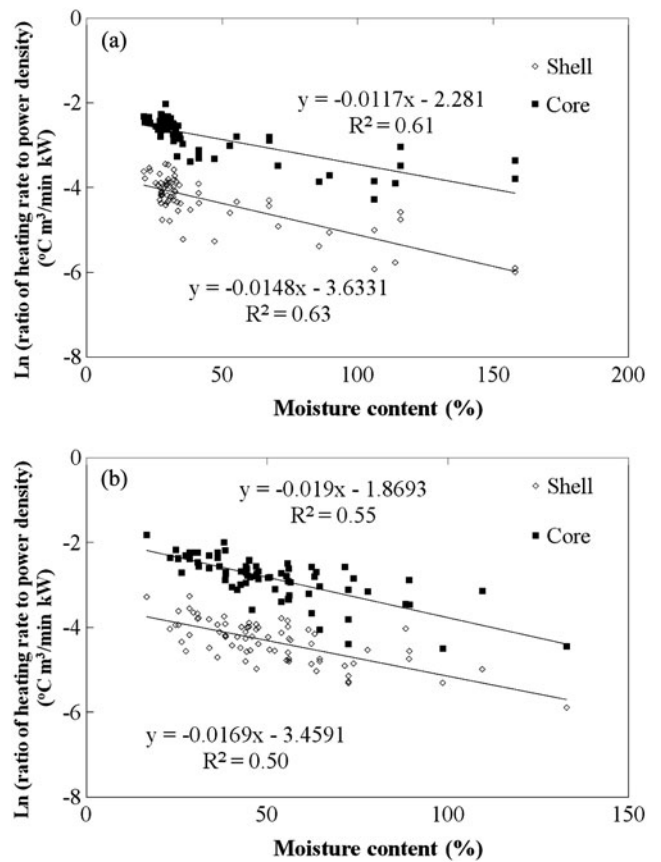The heating rate for each pine specimen was estimated using the developed model. To verify the accuracy of the developed model, the estimated heating rate plotted as a function of experimentally measured heating rate of shell (a) and core (b) is shown in Fig. 6. It is apparent that the correlation between the model and experiment was poor in heating rate of shell and core with R^2 value of 0.20 and 0.36, respectively. This resulted from the assumption that power density was uniform within each specimen. Indeed, closer observation of the initial slope depicted in Fig. 1 shows that the initial slope of core was larger than that of shell. This implies that the power density of core was higher than that of shell, since there is no heat conduction initially and initial slope is equivalent to power density (Antti and Perré 1999). The difference of power density between shell and core might be explained by the dielectric loss factor. The dielectric loss factor is positively correlated to moisture content (Zhou and Avramidis 1999). Then initial moisture content of core is generally higher than that of shell, resulting in a higher dielectric loss factor in core compared with shell. Therefore the power density of core is higher than that of shell, even though electric field is constant along the horizontal direction in a cross section that is the interest in the developed model.
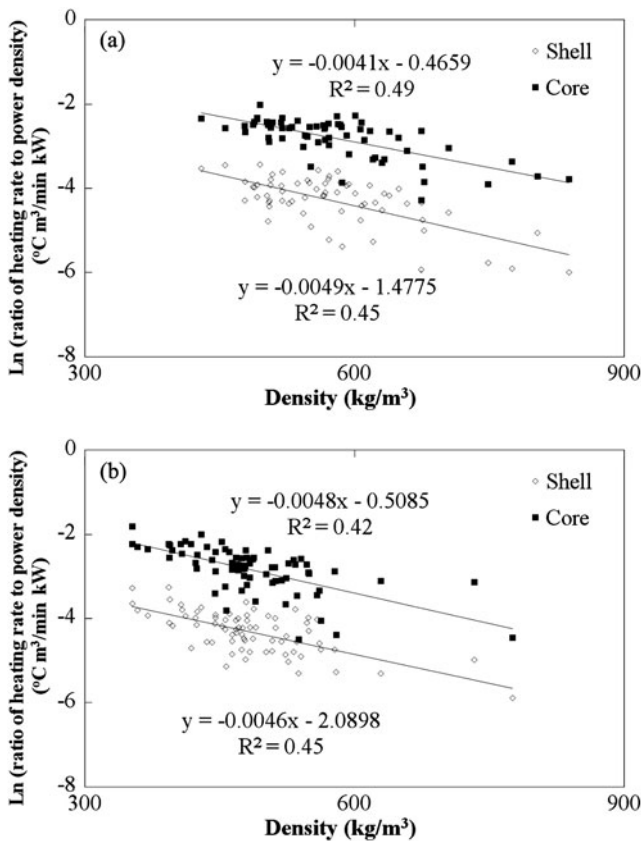
Fig. 7 Measured vs. estimated heating rate of lodgepole pine in shell (**a**) and core (**b**) developed by local power density of shell and core. Solid and dotted lines are regression and trend lines, respectively
Abb. 7 Gemessene Aufheizrate in Abhängigkeit der geschätzten Aufheizrate bei Lodgepole Kiefer im (**a**) äußeren und (**b**) inneren Querschnittsbereich, hergeleitet von der örtlichen Leistungsdichte im äußeren und inneren Querschnittsbereich. Die gestrichelten Linien sind Regressionsgeraden

shell and core was calculated and employed to the developed model, instead of using set power density given by the meter. The model developed using local power density exhibited a strong correlation between estimated and measured heating rate in both shell and core with R^2 value of 0.71 and 0.93, respectively (Fig. 7). The standard error in shell and core was also 0.44 and 0.48, respectively, demonstrating that the developed model was able to predict heating rate of wood with various moisture content under the known power density distribution.

4 Conclusion

Heating rate of wood with various moisture content and power density during RF heating was investigated. Heating rate was positively correlated with power density and negatively correlated with moisture content. The ratio of heating rate to power density is a useful parameter to cancel the influence of the latter. The derived empirical equations made possible the calculation of the heating rate within test conditions applied to this study.

One dimensional mathematical model to describe the heating rate of wood during RF heating was developed. The developed model using local power density showed a strong correlation between estimated and measured heating rate in both shell and core, indicating that the model was able to predict heating rate of wood with various moisture content under the known power density distribution. Calculating power density distribution will be examined in future research.

Fig. 5 Relationship between density and the ratio of heating rate to power density of lodgepole pine (**a**) and western red cedar (**b**)
Abb. 5 Beziehung zwischen Dichte und dem Verhältnis von Aufheizrate zu Leistungsdichte bei (**a**) Lodgepole Kiefer und (**b**) Western Red Cedar
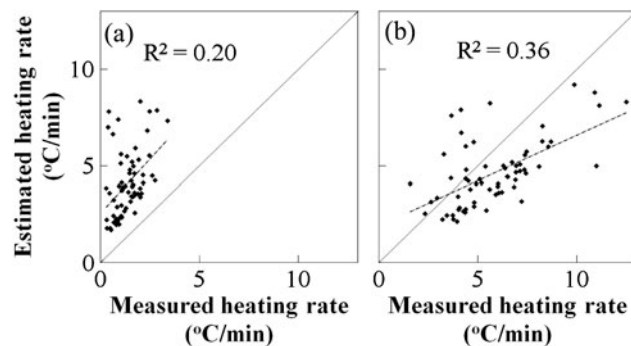

Fig. 6 Measured vs. estimated heating rate of lodgepole pine in shell (**a**) and core (**b**). Solid dotted lines are regression and trend lines, respectively
Abb. 6 Gemessene Aufheizrate in Abhängigkeit der geschätzten Aufheizrate bei Lodgepole Kiefer im (**a**) äußeren und (**b**) inneren Querschnittsbereich. Die gestrichelten Linien sind Regressionsgeraden

To compensate for the difference of power density between shell and core, the initial slope of shell and core for each specimen was obtained from the temperature evolution. Substituting the slope into (2), the local power density of
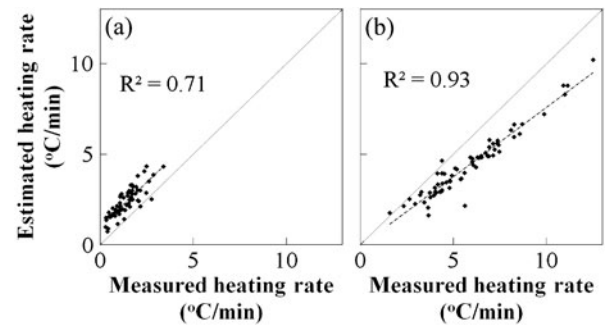
References

Antti AL, Perré P (1999) A microwave applicator for on line wood drying: temperature and moisture distribution in wood. Wood Sci Technol 33:123–138

Avramidis S, Liu F, Neilson BJ (1994) Radio-frequency/vacuum drying of softwoods: drying of thick western red cedar with constant electrode voltage. For Prod J 44(1):41–47

Dwinell LD, Avramidis S, Clark JE (1994) Evaluation of a radio frequency/vacuum dryer for eradicating the pinewood nematode in green, sawn wood. For Prod J 44(4):19–24

Fang F, Ruddick J, Avramidis S (2001) Application of radio-frequency heating to utility poles. Part 3. The use of RF heating to eradicate decay fungi in pole material. For Prod J 51(11/12):51–55

Fleming MR, Hoover K, Janowiak JJ, Fang Y, Wang X, Liu W, Wang Y, Hang X, Agrawal D, Mastro VC, Lance DR, Shield JE, Roy R (2002) Microwave irradiation of wood packing material to destroy the Asian longhorned beetle. For Prod J 52(11/12):1–7

Fleming MR, Janowiak JJ, Kearns J, Shield JE, Roy R, Agrawal DK, Bauer LS, Miller DL, Hoover K (2004) Parameters for scale-up of lethal microwave treatment to eradicate cerambycid larvae infesting solid wood packing materials. For Prod J 54(7/8):80–84

Food and Agriculture Organization (FAO) of the United Nations (2002) Guidelines for regulating wood packaging material in international trade. Inter standards for phytosanitary measures No 13 (ISPM 15), FAO of the United Nations, Rome, S 14

Henin J, Charron S, Luypaert PJ, Jourez B, Hébert J (2008) Strategy to control the effectiveness of microwave treatment of wood in the framework of the implementation of ISPM 15. For Prod J 58(12):75–81

Itoh K (2004) Basis for countermeasures against heat and heat calculation technique. Denshizairyo 4:1–8 (in Japanese)

Khalifa AN (2001) Natural convective heat transfer coefficient—a review I. Isolated vertical and horizontal surfaces. Energy Convers Manage 42:491–504

Koumoutsakos A, Avramidis S, Hatzikiriakos S (2001a) Radio frequency vacuum drying of wood. I. Mathematical model. Dry Technol 19(1):65–84

Koumoutsakos A, Avramidis S, Hatzikiriakos S (2001b) Radio frequency vacuum drying of wood. II. Experimental model evaluation. Dry Technol 19(1):85–98

Lazarescu C, Plattner A, Hart F, Breuil C, Avramidis S (2009) Pasteurization of hemlock by radio frequency heating: a preliminary study. For Prod J 59(4):79–83

Nelson SO, Kraszewski AW (1990) Dielectric properties of materials and measurement techniques. Dry Technol 8(5):1123–1142

Nzokou P, Tourtellot S, Kamdem DP (2008) Kiln and microwave heat treatment of logs infested by the emerald ash borer (*Agrilus planipennis* Fairmaire) (Coleoptera: Buprestidae). For Prod J 58(7/8):68–72

Perré P, Turner IW (1997) Microwave drying of softwood in an over-sized waveguide: theory and experiment. AIChE J 43(10):2579–2595

Perré P, Turner IW (1999) The use of numerical simulation as a cognitive tool for studying the microwave drying of softwood in an over-sized waveguide. Wood Sci Technol 33:445–464

Perrings C, Dehnen-Schmutz K, Touza J, Williamson M (2005) How to manage biological invasions under globalization. Trends Eco Evol 20(2):133–136

Shida S (1993) Utilization and evaluation of exterior wood. III. Two-dimensional difference calculus analysis of a wooden deck's heat-transfer under solar radiation. Mokuzai Gakkaishi 38(1):13–19 (in Japanese)

Simpson W, TenWolde A (1999) Physical properties and moisture relations of wood (Chap 3). In: Wood handbook: wood as an engineering material. General Technical Report FPL-GTR-113, US Department of Agriculture (USDA), Forest Service, Forest Products Laboratory, Madison, WI

Tkacz BM (2002) Pest risks associated with importing wood to the United States. Can J Plant Pathol 24(2):111–116

Torgovnikov GI (1993) Dielectric properties of wood and wood-based material. Springer, Berlin

Tubajika KM, Jonawiak JJ, Mack R, Hoover K (2007) Efficacy of radio frequency treatment and its potential for control of sapstain and wood decay fungi on red oak, poplar, and southern yellow pine wood species. J Wood Sci 53:258–263

United Nations Environment Programme (UNEP) (2000) The Montreal protocol on substances that deplete the ozone layer. Ozone Secretariat, UNEP, Nairobi, Kenya. Available via DIALOG. http://ozone.unep.org/pdfs/Montreal-Protocol2000.pdf. Accessed 17 May 2009

Work TT, MacCullough DG, Cavey JF, Komsa R (2005) Arrival rate of nonindigenous insect species into the United States through foreign trade. Biol Invasions 7(2):323–332

Zhou B, Avramidis S (1999) On the loss factor of wood during radio frequency heating. Wood Sci Technol 33:299–310